Dominance of γ-γ electron-positron pair creation in a plasma driven by high-intensity lasers: Supplemental Material

Yutong He[1], Thomas G. Blackburn[2], Toma Toncian[3], and Alexey V. Arefiev[1,*]

[1]University of California at San Diego, La Jolla, California 92093, USA
[2]Department of Physics, University of Gothenburg, SE-41296 Gothenburg, Sweden
[3]Institute for Radiation Physics, Helmholtz-Zentrum Dresden-Rossendorf e.V., 01328 Dresden, Germany

Supplementary Note 1. Channel density scan

In our simulations, the electron density in the channel is set at $n_{\rm ch} = (a_0/100)3.8n_{\rm c}$. This value was chosen to achieve prolonged laser propagation inside the channel, such that each laser pulse can generate ultrarelativistic electrons without becoming significantly depleted prior to the collision. In order to show that the observed trend is valid for a range of channel densities, we have performed channel density scans for $a_0 = 160$ and $a_0 = 190$. The pair yield for the linear and nonlinear Breit-Wheeler processes is given in Supplementary Table 1 for $a_0 = 160$ and in Supplementary Table 2 for $a_0 = 190$. The ratio of the linear to nonlinear pair yield increases for $0.8 \le n_{\rm e}/n_{\rm ch} \le 1.2$ as we reduce a_0 from 190 to 160. This is the trend that is reported in the main text, which indicates that our observations apply to a range of channel densities and no fine-tuning is necessary.

Supplementary Table 1. Number of pairs at $a_0 = 160$ for different electron densities, $n_{\rm e}$, in the channel. The density $n_{\rm e}$ is given in terms of $n_{\rm ch} = (a_0/100)3.8n_{\rm c}$, where $n_{\rm c}$ is the critical density.

$n_{\rm e}/n_{\rm ch}$	0.8	1.0	1.2
Linear BW pairs ($\times 10^8$)	5.89	6.05	6.21
Nonlinear BW pairs ($\times 10^8$)	1.06	0.86	0.38

Supplementary Table 2. Number of pairs at $a_0 = 190$ for different electron densities, $n_{\rm e}$, in the channel. The density $n_{\rm e}$ is given in terms of $n_{\rm ch} = (a_0/100)3.8n_{\rm c}$, where $n_{\rm c}$ is the critical density.

$n_{\rm e}/n_{\rm ch}$	0.8	1.0	1.2
Linear BW pairs ($\times 10^8$)	17.0	13.1	11.8
Nonlinear BW pairs ($\times 10^8$)	9.2	6.6	4.4

Supplementary Note 2. Distribution of nonlinear Breit-Wheeler pairs

Supplementary Figure 1 provides additional information on the production of nonlinear Breit-Wheeler pairs. The horizontal scale shows the emission time, $t_{\rm emit}$, of energetic photons that go on to produce pairs by interacting with the laser photons. The energetic photons are generated and subsequently propagated as particles by the PIC code. The time of the pair production, $t^{\rm BW}_{\rm nonlin}$, is shown along the vertical scale. The number of pairs for each pairing of $t_{\rm emit}$ and $t^{\rm BW}_{\rm nonlin}$ is color-coded. The pair production is directly computed by the PIC code. The numbers shown in the figure are obtained by assuming that the spatial scale along the z axis is equal to the initial width of the channel.

The vast majority of the nonlinear pairs are produced by photons emitted after the two lasers collide. Indeed, $t_{\rm emit} = 0$ is the time when the two laser beams begin to collide. Most of the pairs are located at $t_{\rm emit} > 0$, which indicates that the parent photons were generated after the collision.

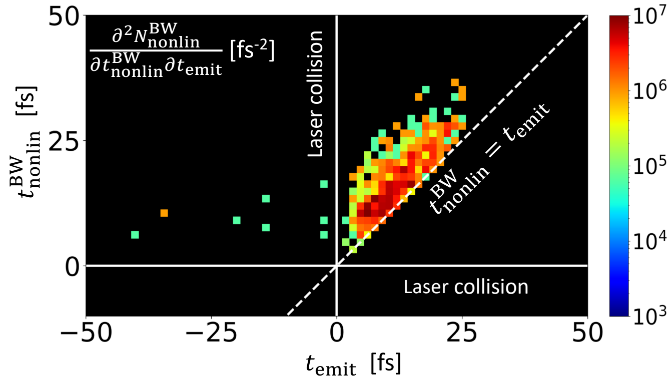

Supplementary Figure 1. Distribution function $\partial^2 N^{\mathrm{BW}}_{\mathrm{nonlin}}/(\partial t^{\mathrm{BW}}_{\mathrm{nonlin}} \partial t_{\mathrm{emit}})$ [fs^{-2}] of the number of electron-positron pairs over the time $t^{\mathrm{BW}}_{\mathrm{nonlin}}$ of pair creation and the t_{emit} of the parent photons. The peak amplitude of each laser peak is $a_0 = 190$.

Supplementary Note 3. Strong-field modifications to the linear Breit-Wheeler cross section

The cross section we use to determine the number of electron-positron pairs created by the linear Breit-Wheeler process, Eq. (1), is calculated assuming that the photons are in vacuum. However, our calculations show that the pairs are created within the plasma channel as the laser pulses overlap, where the background electromagnetic field is strong. The presence of a strong magnetic field[1,2] or plane EM wave is known to modify the cross section for this process. Calculations of the cross section in the latter case have focused on changes at moderate a_0[3] or on resonance features[4,5]. Resonances occur where the intermediate fermion is on mass shell, which corresponds to the incoherent combination of nonlinear pair creation, followed by photon absorption by one of the daughter fermions, in the high-intensity regime. This contribution, which is effectively driven by a single photon, is already counted as our simulations include nonlinear pair creation; photon absorption by an electron in a strong field[6,7] is suppressed unless the photon and electron are aligned within electron's emission cone. (See supporting simulations by Blackburn et al.[8])

As such, in order to estimate the effect of the strong field at $a_0 \gg 1$, we use the cross section for two-photon pair creation in a constant, crossed field given by Baier et al.[9] (see Sec. 5.7). If two-photon pair creation is kinematically allowed, i.e. $\varsigma > 1$, corrections to the cross section scale as $(\chi_\gamma/\varsigma)^2$, where χ_γ is the quantum nonlinearity parameter[9]: in the scenario under consideration here, the photons which undergo linear pair creation have MeV energies and $\chi_\gamma \ll 1$, and therefore these corrections can be neglected. On the other hand, the fact the laser-plasma interactions provide a platform for prolific two-photon pair creation in a region of strong EM field, as our results show, motivates a more general treatment that can investigate where these field-driven corrections become substantial. We note that a related process, pair annihiliation to two photons in a pulsed, plane EM wave, has recently been revisited[10].

Supplementary Note 4. Pair production algorithm for head-on collisions of beamlets

Our algorithm for computing the pair production yield due to the linear Breit-Wheeler process leverages the fact that the colliding photons are emitted over an extended period of time compared to the characteristic travel time between the emission locations. In what follows, we illustrate its implementation for head-on collisions of two beamlets. Near head-on collisions are the biggest contributor to the pair yield and this is also the regime that greatly benefits from our simplified approach in terms of computational efficiency.

We are considering a head-on collision of two counterpropagating beamlets that have the same transverse area S. The first beamlet is being emitted at $x = x_1$ and it propagates in the positive direction. It is convenient to use the emission time τ as a marker for the photons in each beamlet. The corresponding photon density in the first beamlet is then $n_1(\tau_1)$. The counterpropagating beamlet is emitted at $x = x_2 > x_1$ and its photon density is $n_2(\tau_2)$. The total pair yield by these two beamlets interacting with each other is

$$\Delta N_{\mathrm{pairs}} = \sigma_{\gamma\gamma} S c^2 \int_{-\infty}^{+\infty} d\tau_1 n_1(\tau_1) \left[\int_{\tau_1 - l/c}^{\tau_1 + l/c} d\tau_2 n_2(\tau_2) \right], \tag{1}$$

where

$$l \equiv x_2 - x_1. \tag{2}$$

Supplementary Equation (1) presents a direct approach to calculating the pair yield and it involves a double integral.

In our case, the typical beamlet emission lasts longer than l/c, which suggests a possible simplification of replacing $n_2(\tau_2)$ with $n_2(\tau_1)$. The inner integral in Supplementary Equation (1) can then be directly evaluated and we find that

$$\Delta N_{\text{pairs}} \approx 2c\sigma_{\gamma\gamma}V\int_{-\infty}^{+\infty} n_1(\tau)n_2(\tau)d\tau, \tag{3}$$

where $V \equiv lS$ is the interaction volume. Note that the two beamlets are interchangeable in this expression. In order to estimate the error, we expand $n_2(\tau_2)$ around $\tau_2 = \tau_1$ and retain linear and quadratic terms in the expansion. The time integral of the linear term in Supplementary Equation (1) is equal to zero, which means that the error in our approach is determined by the quadratic term. We thus estimate that the relative error in the number of produced pairs scales as $(l/c\Delta\tau)^2$, where $\Delta\tau$ is the characteristic duration of beamlet emission.

We compute the spatial distribution of pairs by simply assigning the pair density

$$\Delta n_{\text{pairs}} = \Delta N_{\text{pairs}}/V \tag{4}$$

to each position within the interaction volume. We call this the *average density method*. A direct approach would however require us to compute the following integral at each position along the x axis:

$$\Delta n_{\text{pairs}}^{\text{direct}}(x) = 2c\sigma_{\gamma\gamma}\int_{-\infty}^{+\infty} n_1(t_1)\,n_2(t_2)\,dt, \tag{5}$$

where

$$t_1 = t - (x - x_1)/c, \tag{6}$$
$$t_2 = t - (x_2 - x)/c. \tag{7}$$

The direct approach is much more demanding computationally.

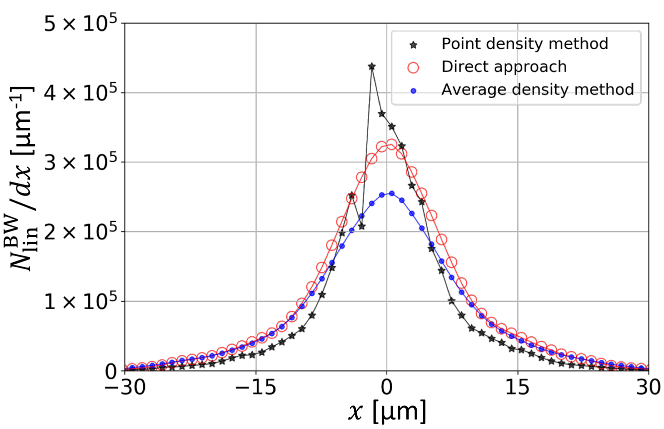

Supplementary Figure 2. Spatial distribution of linear Breit-Wheeler pairs produced in a head-on collision of spatially distributed beamlets. The three curves represent three different approaches: direct approach (open circles), average density method (solid circles), and point density method (star markers).

Even though our approach for calculating the spatial distribution of pairs is deliberately crude for a single pair of beamlets, it is effective when applied to a large ensemble of spatially distributed beamlets. As an example, we have carried out calculations for approximately 3000 spatially distributed beamlets, where 1573 beamlets are directed to the right and 1590 beamlets are directed to the left. The photon energy range is 0.19 MeV $< \varepsilon_\gamma <$ 2.05 MeV. We used our PIC simulation to generate these beamlets by selecting photons emitted with $|\theta| < 5.15^\circ$ or $|\theta - \pi| < 5.15^\circ$. The average density method that uses Δn_{pairs} from Supplementary Equation (4) for each beamlet-beamlet collision gives the curve shown with small solid circles. The direct approach detailed by Supplementary Equation (5) gives the curve shown with open circles. The two curves have a similar shape, but the direct approach took almost two orders of magnitude longer in terms of computational time. The relative difference in the total number of pairs between the two methods is less than 17%.

Our method evenly distributes the generated pairs over the interaction volume, which is the key to achieving a good agreement with the direct but more computationally expensive approach. In order to illustrate this aspect, we performed another calculation. In this case, all of the pairs produced by two beamlets are placed into the center of the interaction volume without being evenly distributed. We call this the *point density method*. The density is calculated as $\Delta N_{\text{pairs}}/S\Delta x$, where ΔN_{pairs} is given by Supplementary Equation (3) and Δx is the thickness of slices that we use for spatial discretization into beamlets. The result of this procedure is shown with star markers in Supplementary Figure 2. There are no significant savings in terms of computational costs compared to the average density method. The characteristic width of the spatial distribution shows considerable deviation from that for the direct approach.

Supplementary References

1. Ng, Y. J. & Tsai, W. Pair creation by photon-photon scattering in a strong magnetic field. *Phys. Rev. D* **16**, 286–294, DOI: 10.1103/PhysRevD.16.286 (1977).

2. Kozlenkov, A. A. & Mitrofanov, I. G. Two-photon production of $e^{\pm}$ pairs in a strong magnetic field. *Sov. Phys. JETP* **64**, 1173–1179 (1986).

3. Denisenko, O. I. The Breit-Wheeler process in the laser field. *Laser Phys.* **18**, 920–924, DOI: 10.1134/S1054660X08070189 (2008).

4. Hartin, A. Strong field QED in lepton colliders and electron/laser interactions. *Int. J. Mod. Phys. A* **33**, 1830011, DOI: 10.1142/S0217751X18300119 (2018).

5. Hartin, A. *Second Order QED Processes in an Intense Electromagnetic Field*. Ph.D. thesis, University of London (2006).

6. Ritus, V. I. Quantum effects of the interaction of elementary particles with an intense electromagnetic field. *J. Sov. Laser Res.* **6**, 497–617, DOI: 10.1007/BF01120220 (1985).

7. Ilderton, A., King, B. & MacLeod, A. J. Absorption cross section in an intense plane wave background. *Phys. Rev. D* **100**, 076002, DOI: 10.1103/PhysRevD.100.076002 (2019).

8. Blackburn, T. G. *et al.* Self-absorption of synchrotron radiation in a laser-irradiated plasma. *Phys. Plasmas* **28**, 053103, DOI: 10.1063/5.0044766 (2021). https://doi.org/10.1063/5.0044766.

9. Baier, V. N., Katkov, V. M. & Strakhovenko, V. M. *Electromagnetic Processes at High Energies in Oriented Single Crystals* (World Scientific, Singapore, 1998).

10. Bragin, S. & Piazza, A. D. Electron-positron annihilation into two photons in an intense plane-wave field (2020). 2003.02231.